Clinical tissue characterization: online determination of magnitude and time delay of myocardial backscatter

3

Joel Mobley, MA, Christina E. Banta, MS, Hiie M. Gussak, MD, Julio E. Perez, MD and James G. Miller, PhD

Implementation of an algorithm for the automated determination of the magnitude and time delay of the cardiac cycle-dependent variation of integrated backscatter is reported. This algorithm has been implemented in the experimental firmware of a commercially-available echocardiographic imaging system. Integrated backscatter and the cardiac cycle-dependent variation (cyclic variation) of integrated backscatter are described and their roles in myocardial tissue characterization are discussed. A brief description of the algorithm used for the determination of the magnitude and time delay is given, followed by accounts of the process of collecting cyclic variation data and the algorithm implementation on the cardiac system. This implementation demonstrates how tissue characterization techniques could be used to augment diagnostic ultrasound and may facilitate the further investigation of the diagnostic potential of the cyclic variation of myocardial backscatter.

INTRODUCTION

An evolving application of ultrasonic examination of the heart is tissue characterization, the goal of which is to classify the health or pathology of myocardial segments based on the intrinsic interaction of ultrasound with the tissue.[1] The specific approach to tissue characterization followed in this work involves the derivation of quantitative parameters from the radio frequency signals received due to the scattering of ultrasound from tissue. These derived parameters should be reproducible and independent of instrumentation. The utilization of tissue characterization methods in a clinical setting requires the rapid determination of these quantitative indices from which the physical state of the tissue in question can be ascertained. In this article, we describe and demonstrate the implementation of an algorithm for the automated determination of the magnitude and time delay of the cardiac cycle-dependent variation of integrated backscatter in experimental firmware on a commercially-available cardiac imaging system. This pilot implementation can facilitate the evaluation of the magnitude and time delay indices as clinically-relevant parameters for tissue characterization and demonstrate the role that tissue characterization can play in augmenting the diagnostic capabilities of clinical ultrasound.

From the Department of Physics and Cardiology Division, Washington University, St. Louis, MO and Hewlett-Packard Co., Andover, MA,

Address for correspondence: James G. Miller, PhD, Laboratory for Ultrasonics, Department of Physics – Box 1105, Washington University, One Brookings Drive, St. Louis, MO 63130-4899.

1052-2174/95 $3.50.

INTEGRATED BACKSCATTER

Integrated backscatter is a measure of the acoustic energy returned to the transmitting transducer due to the scattering of the ultrasound by a tissue segment. For the purposes of myocardial tissue characterization, the acoustic backscatter signals of interest are those emanating from the intramural myocardium, avoiding signals due to tissue boundaries (i.e., blood-tissue or tissue-pericardial interfaces). This scattering of ultrasound by intramural myocardium is due to the small-scale differences in the mechanical properties among the material constituents of the tissue. The determination of integrated backscatter from the raw signal backscattered by tissue is a multistep process. First, a gate is used to isolate the portion of the signal that is due to

the backscatter from the tissue of interest. This gated signal represents the scattering from a volume of tissue that is defined by the length of the gate and the effective cross-sectional area of the insonifying ultrasonic beam. In one approach, a Fourier decomposition of this gated signal is performed. This allows the determination of the signal's power spectrum, i.e., the acoustic power backscattered to the transducer as a function of the respective temporal frequencies that comprise the signal. (An alternate approach to determining integrated backscatter using only time-domain techniques is described in the accompanying video).

In order to determine the absolute level of energy contained in the signal, its power spectrum is normalized by the spectrum from a reference of known backscatter strength, usually an ultrasonic mirror such as a steel plate in water. The resulting power curve is then averaged (i.e., integrated) over the usable frequency range of the signal to obtain the integrated backscatter value. This averaging over frequency serves to minimize the influences of interference and phase cancellation effects that arise due to the presence of many scattering sites within the interrogated tissue volume.

Typically, the integrated backscatter values from nearby insonified tissue volumes are averaged to obtain a single value over some localized region. The spatial extent of the region will depend on the center frequency of the transmitted ultrasound. For clinical scanners, where the center frequency is in the 2 to 5 MHz range, the extent of spatial averaging used is on the order of several millimeters in each direction. This technique of spatial averaging, while reducing localization somewhat, aids significantly in making the measurements stable and reproducible.

In vitro and *in vivo* studies of both animal and human hearts have shown that integrated backscatter and other related acoustic indices differentiate among acutely ischemic tissue, old infarct and normal tissue, and correlate with collagen content and other measures of tissue state.[2-25] Studies of humans have also shown that integrated backscatter can be used to delineate blood-tissue boundaries in real-time, facilitating online analysis of cavity areas and volumes during echocardiographic examination.[26-28]

CYCLIC VARIATION OF INTEGRATED BACKSCATTER

In addition to the correlation of absolute integrated backscatter (i.e., normalized by some reference scatterer or reflector) with tissue properties, the integrated backscatter from myocardium is observed to undergo a characteristic variation over the cardiac cycle.[29-32] This pattern of cyclic variation is characterized by two distinct regimes over the heart cycle. In general, the integrated backscatter level approximates a relative maximum value for the majority of the cycle and falls to a minimum level, or trough, for a time duration roughly equivalent to the systolic interval (Fig. 1). The position of this trough in the variation relative to the heart cycle can vary depending on the details of the acquisition and the state of the insonified tissue. Changes in the pattern of cyclic variation have been correlated with changes in cardiac function and specific pathologic myocardial states.[33-39] In order to yield quantitative comparisons, cyclic variation data are characterized by two parameters, the magnitude and time delay. The magnitude is a measure of the difference in the respective average integrated backscatter values between the minimum and maximum levels of the variation (Fig. 2). Because integrated backscatter values are expressed on a decibel (dB) scale, the magnitude is similarly expressed in decibels. The time delay begins as a measure of the time

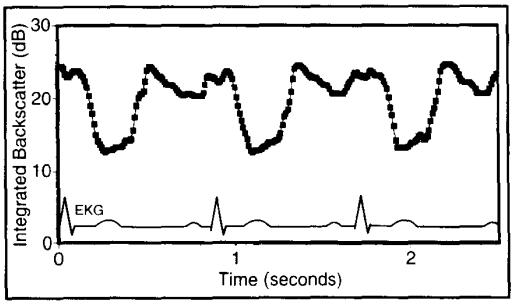

Fig. 1 Cyclic variation of integrated backscatter over three heart cycles. This data set illustrates the two-level pattern that is characteristic of cyclic variation. For the majority of each heart cycle, the backscatter fluctuates about a baseline value and then dips into a "trough" or minimum level for a period of time on the order of the systolic interval. This data was collected from the left-ventricular posterior wall of a normal human volunteer using an echocardiographic imaging system with real-time integrated backscatter processing.

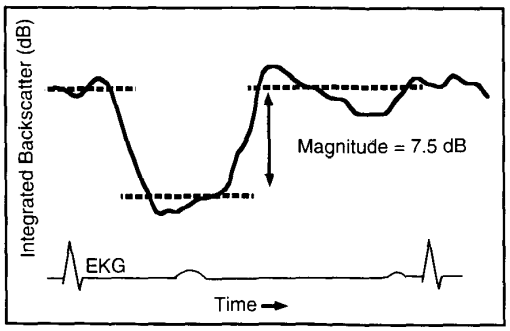

Fig. 2 Magnitude of cyclic variation. The magnitude is a measure of the size of the primary variation in the integrated backscatter data over the heart cycle. The magnitude is determined by taking the difference between the average integrated backscatter levels of the baseline region and the trough, respectively.

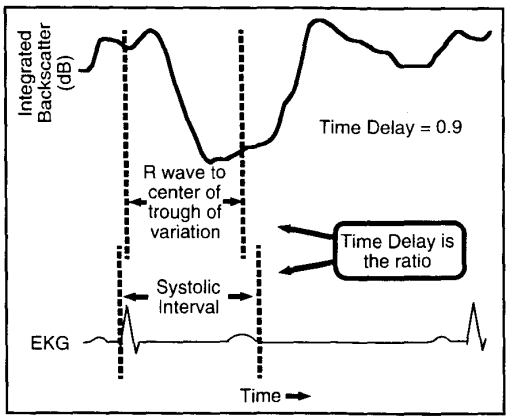

Fig. 3 Time delay of cyclic variation. The time delay measures the offset of the center of the trough of variation from the R wave of the EKG. This time interval is then normalized by the systolic interval to arrive at the dimensionless time delay.

interval from the R-wave of a simultaneously-recorded EKG to the center of the minimum-value phase of the variation curve. This time interval is then normalized (i.e., divided) by the systolic interval to yield a dimensionless parameter (Fig. 3). Many studies in both humans and experimental animals have shown correlation between the cyclic variation parameters and physical state of the tissue.[8,21,25,33-37,40-55] One such study in dogs showed that the magnitude and time delay values return to normal faster than the recovery of wall thickening during the reperfusion of previously ischemic but viable tissue.[56] Transthoracic studies in humans have also shown that magnitude and time delay of cyclic variation can distinguish between normal and infarcted tissue as well as normal and acutely ischemic tissue.[42,45,47,57] A further study has also suggested that the magnitude and delay of the cyclic variation may be a more sensitive indicator than conventional echocardiographic measurements for the detection of the onset of diabetic heart disease.[49] Because the quantitative analysis of cyclic variation data only requires the consideration of relative changes in integrated backscatter rather than its absolute determination, it is particularly attractive for use in situations where ascertaining absolute levels of backscatter may be difficult.[58-60]

Initial investigations of the cyclic variation showed a maximum in integrated backscatter to occur near end-diastole and a minimum to occur at end-systole. This observation led to the use of a two-point analysis of cyclic variation in which integrated backscatter values near end-diastole and end-systole were taken as maximum and minimum values of the backscatter curve. This method of analysis resulted in a magnitude-only parameterization of cyclic variation, with no explicit recognition of the timing aspects of the variation. However, subsequent work has shown that this relationship strictly held only under specific conditions. Thus, the two-point end-systolic/end-diastolic method of analysis is inadequate for several reasons. Due to the organization of its muscle fibers, the heart has anisotropic acoustic properties, i.e., the interaction of ultrasound and myocardium depends on the angle of incidence of the sound beam relative to the orientation of the myofibers.[9,43,61-68] Thus, the amount of backscatter produced by a tissue segment depends on the direction from which it is insonified. Recent work suggests that normal myocardium exhibits anisotropy in its pattern of cyclic variation as well.[69-71] This work shows that the minimum and maximum levels of the cyclic variation pattern from healthy segments are not always coincident with end-systole and end-diastole, respectively, for directions of insonification parallel or oblique to local myofibers. The state of health of the tissue under study also influences the position of the two levels in the variation curve relative to the cardiac cycle. Furthermore, the use of only two points from the backscatter curve for measurement purposes is

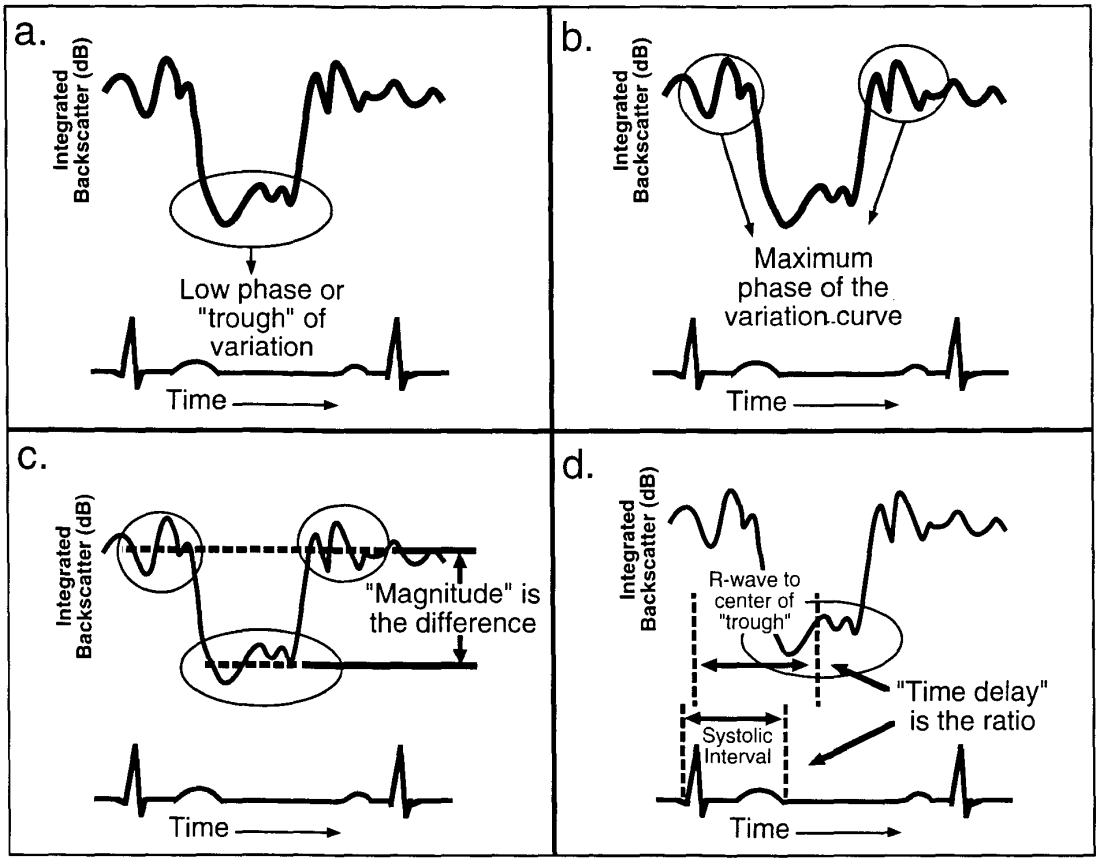

Fig. 4 Interpretation of cyclic variation data. (a) Identification of the low phase (or trough) of the cyclic variation curve. This is the portion of the curve that, on average, lies below the mean backscatter level over the heart cycle. (b) Identification of the maximal portion of the curve. This is the portion of the curve that, on average, lies above the mean backscatter level over the heart cycle. (c) Average backscatter values over the two regions are determined. The magnitude of variation is the difference in the two average integrated backscatter values. (d) Time delay determination begins by finding the time interval from the R-wave of the EKG to the center of the trough of the variation. This interval is then divided by the time duration of systole to complete the time delay calculation.

more susceptible to measurement noise and small scale variations than a quantitative analysis that employs the entire data curve to extract the size of the primary variation. Also, the explicit inclusion of the timing information, which we quantify as the normalized time delay, complements the magnitude parameterization of the cyclic variation data augmenting its diagnostic potential.[72] Thus, we advocate the interpretation of cyclic variation data by identifying the following features of the integrated backscatter versus time curve: (1) a region of the curve with a time duration on the order of the systolic interval for which the backscatter values fall below the mean value of the entire data set; and (2) the region of the data set where the data lie above the mean data set value. After identification, the average integrated backscatter value for each region is determined and the absolute difference between the two levels is then the magnitude of variation for the data. Additionally, the position in time of the center of the region of reduced backscatter relative to end-diastole is determined. This time interval is divided by the systolic interval duration to determine the time delay (Fig. 4).

In general, abnormal myocardium exhibits a decrease in magnitude and an increase in time delay in comparison with healthy tissue. The range of values for normal tissue varies depending on the segment insonified and the direction of interrogation. Typical values for the magni-

tude and time delay of normal myocardium imaged in standard echocardiographic views have been reported by Finch-Johnston et al.[70]

ALGORITHM FOR DETERMINING MAGNITUDE AND TIME DELAY OF CYCLIC VARIATION

In order to permit an objective analysis of cyclically-varying integrated backscatter data, an algorithm was developed for the automated extraction of the magnitude and time delay.[73] In addition to the variation curve, the algorithm also requires some independent indicator of the timing of the cardiac cycle relative to the backscatter data, which can be provided by a simultaneously-recorded EKG. An idealized model of the variation is employed to determine the parameters. This model exhibits two integrated backscatter levels over the heart cycle, with the duration of the minimum level equivalent to the systolic interval (as approximated by the QT interval from the EKG). The initial values for the two levels of the model function are chosen such that the model has a zero average over the heart cycle and a magnitude (difference in integrated backscatter value between the two levels) of unity. These specific choices are made to avoid complications in the time delay determination and to simplify the magnitude calculations. Using Fourier analysis, the amplitude of variation of the model is compared with that of the backscatter data, resulting in the extraction of the magnitude. By performing a cross-correlation, the position of the minimum phase of the model is adjusted to best fit the data. This operation in concert with timing information from the EKG (position of R-wave and length of QT interval) yields the necessary input to determine the time delay parameter. Earlier versions of the algorithm have undergone validation tests, pitting the best manual estimates versus the automated determinations of the magnitude and time delay.[73,74] These studies have confirmed the utility and accuracy of the algorithm. However, in a fraction of the cases studied, the algorithm produced clear overestimates of the magnitude.[75] The latest version of the algorithm, demonstrated in the accompanying video, includes an additional step in the magnitude determination that extends its applicability to a broader range of cyclic variation data. This current version can detect the special conditions under which the older reported versions[73,74] would produce overestimates of the magnitude. When these conditions are present, this updated algorithm implements a correction procedure that results in a significantly more accurate magnitude determination.

IMPLEMENTATION AND USE OF ALGORITHM ON A MEDICAL IMAGING SYSTEM

The algorithm has been implemented in experimental firmware on the Hewlett-Packard SONOS 1500™ cardiac imaging system. The real-time integrated backscatter processing capability of that system allows for the online acquisition of integrated backscatter data as a function of time. In contrast with the frequency domain (Fourier transform) method described above, the system employs a time-domain sum-of-squares approach to the estimation of integrated backscatter using an integration time of 3.2 μm.[76,77] (For more detail on the time-domain approach and real-time integrated backscatter. see the accompanying video). The algorithm resides within the M-mode integrated backscatter operating environment of the system. In this operating environment, the system produces M-mode images in which each pixel has an assigned integrated backscatter value. To begin the data acquisition process, the operator selects a specific line from the two-dimensional sector image that intersects the tissue segment of interest. This line is then used in M-mode to form the desired real-time integrated backscatter images. The system can hold approximately 30 seconds of M-mode integrated backscatter image data. An EKG is displayed and recorded along with the image data. Once the operator has acquired satisfactory images, several heart cycles are selected out of the many obtained for the generation of the cyclic variation data. After the cycles of interest are chosen and displayed on-screen, the operator moves a region-of-interest cursor (ROI) through the M-mode representation of the myocardial tissue segment under investigation. All of the integrated backscatter

values assigned to the image pixels that fall within the ROI are averaged, producing a single integrated backscatter value. The ROI is square in shape and its size can be varied. The size is chosen to be as large as possible, to achieve good spatial averaging, while staying entirely within the myocardium to avoid corruption from specular reflections at the tissue boundaries. An integrated backscatter trace is then simultaneously acquired and plotted on-screen by driving the ROI, via a trackball, through the image of the segment of interest.

Once the integrated backscatter data is obtained, the algorithm process can be activated. The operator confirms that the algorithm processing is active and selects the number of consecutive heart cycles of the data that they wish to analyze. Once the preliminary settings are approved, the operator begins the process of entering the timing information. Using the cursor under trackball control, the operator enters the timing information by marking the following locations on the EKG for the consecutive heart cycles to be analyzed: onset of QRS, end of T-wave, and the R-wave. In addition, the QRS following the last cycle of interest is marked to frame the data of interest. After the timing markers have been set and approved, the calculations of the cyclic variation parameters begin. At the conclusion of the calculations, the results for the magnitude and time delay are displayed automatically in a results window and the computed model fit is superimposed on the displayed integrated backscatter data plot.

The implementation reported here is expected to facilitate the evaluation of the magnitude and time delay indices as clinically relevant parameters for tissue characterization. It is hoped that these efforts will help to establish myocardial tissue characterization as a complement to diagnostic echocardiography that can be readily performed at the ambulatory patient lab or at the bedside of critically-ill patients with myocardial dysfunction.

REFERENCES

1. For a review of cardiac tissue characterization using ultrasound, see: Skorton DJ, Miller JG, Wickline S, Barzilai B, Collins SM, Perez JE. Ultrasonic characterization of cardiovascular tissue. In: Marcus ML, Schelbert HR, Skorton DJ, Wolf GL and Braunwald E, ed. Cardiac Imaging: A Companion to Braunwald's Heart Disease. Philadelphia: W. B. Saunders Company, 1991: 538-556, Chapter 26.

2. O'Donnell M, Bauwens D, Mimbs JW, Miller JG. Broadband integrated backscatter: an approach to spatially localized tissue characterization *in vivo*. Proc IEEE Ultrason Symp 1979;79 CH 1482-9:175-8.

3. Perez JE, Barzilai B, Madaras EI, et al. Applicability of ultrasonic tissue characterization for longitudinal assessment and differentiation of calcification and fibrosis in cardiomyopathy. J Am Coll Cardiol 1984;4:88-95.

4. Mimbs JW, O'Donnell M, Miller JG, Sobel BE. Detection of cardiomyopathic changes induced by doxorubicin based on quantitative analysis of ultrasonic backscatter. Am J Cardiol 1981;47:1056-60.

5. Mimbs JW, Bauwens D, Cohen RD, O'Donnell M, Miller JG, Sobel BE. Effects of myocardial ischemia on quantitative ultrasonic backscatter and identification of responsible determinants. Circ Res 1981;49:89-96.

6. Cohen RD, Mottley JG, Miller JG, Kurnik PB, Sobel BE. Detection of ischemic myocardium *in vivo* through the chest wall by quantitative ultrasonic tissue characterization. Am J Cardiol 1982;50:838-43.

7. Wickline SA, Thomas LJ III, Miller JG, Sobel BE, Perez JE. A relationship between ultrasonic integrated backscatter and myocardial contractile function. J Clin Invest 1985;76:2151-60.

8. Barzilai B, Thomas LJ III, Glueck RM, et al. Detection of remote myocardial infarction with quantitative real-time ultrasonic characterization. J Am Soc Echo 1988;1:179-86.

9. Mottley JG, Miller JG. Anisotropy of the ultrasonic backscatter of myocardial tissue: I. theory and measurements *in vitro*. J Acoust Soc Amer 1988;83:755-61.

10. Wickline SA, Verdonk ED, Miller JG. Three-dimensional characterization of human ventricular myofiber architecture by ultrasonic backscatter. J Clin Invest 1991; 88:438-46.

11. Wickline SA, Verdonk ED, Wong AK, Shepard RK, Miller JG. Structural remodeling of human myocardial tissue after infarction. Circ 1992;85:259-68.

12. Baello EBJ, McPherson DD, Conyers DJ, Collins SM, Skorton DJ. Ultrasound study of acoustic properties of the normal canine heart: comparison of backscatter from all chambers. J Am Coll Cardiol 1986;8:880-4.

13. Haendchen RV, Ong K, Fishbein MC, Zwehl W, Meerbaum S, Corday E. Early differentiation of infarcted and noninfarcted reperfused myocardium in dogs by quantitative analysis of regional myocardial echo amplitudes. Circ Res 1985;57:718-28.

14. Hoyt RM, Skorton DJ, Collins SM, Hewlett E. Melton J. Ultrasonic backscatter and collagen in normal ventricular myocardium. Circ 1984;69:775-82.

15. Hoyt RH, Collins SM, Skorton DJ, Ericksen EE, Conyers D. Assessment of fibrosis in infarcted human hearts by analysis of ultrasonic backscatter. Circ 1985;71: 740-4.

16. Lattanzi F, Bellotti P, Picano E, et al. Quantitative ultrasonic analysis of myocardium in patients with thalassemia major and iron overload. Circ 1993;87:748-54.

17. Naito J, Masuyama T, Tanouchi J, et al. Analysis of transmural trend of myocardial integrated ultrasound backscatter for differentiation of hypertrophic cardiomyopathy and ventricular hypertrophy due to hypertension. J Am Coll Cardiol 1994;24:517-24.

18. Picano E, Faletra F, Marini C, Paterni M, et al. Increased echodensity of transiently asynergic myocardium in humans: a novel echocardiographic sign of myocardial ischemia. J Am Coll Cardiol 1993;21:199-207.

19. Pingitore A, Kozakova M, Picano E, Paterni M, Landini L, Distante A. Acute myocardial gray level intensity changes detected by transesophageal echocardiography during intraoperative ischemia. Am J Cardiol 1993; 72:465-9.

20. Rasmussen S, Lovelace DE, Knoebel SB, Ransburg R, Corya BC. Echocardiographic detection of ischemic and infarcted myocardium. J Am Coll Cardiol 1984;3:733-43.

21. Rhyne TL, Sagar KB, Wann SL, Haasler G. The myocardial signature: absolute backscatter, cyclical variation, frequency variation, and statistics. Ultrasonic Imaging 1986;8:107-20.

22. Rijsterborgh H, Mastik F, Lancee CT, et al. Ultrasonic myocardial integrated backscatter and myocardial wall thickness in animal experiments. Ultrasound Med Biol 1990;16:29-36.

23. Rijsterborgh H, Mastik F, Lancee CT, et al. The relative contributions of myocardial wall thickness and ischemia to ultrasonic myocardial integrated backscatter during experimental ischemia. Ultrasound Med Biol 1991; 17:41-8.

24. Skorton DJ, Melton HE, Pandian NG, et al. Detection of acute myocardial infarction in closed chest dogs by analysis of regional two-dimensional echocardiographic gray-level distributions (abstr). Circ Res 1983;52:36.

25. Vandenberg BF, Kieso RA, Fox-Eastham K, et al. Characterization of acute experimental left ventricular thrombi with quantitative backscatter imaging. Circ 1990;81: 1017-23.

26. Perez JE, Waggoner AD, Barzilai B, Melton HE, Miller JG, Sobel BE. On-line assessment of ventricular function by automatic boundary detection and ultrasonic backscatter imaging. J Am Coll Cardiol 1992;19:313-20.

27. Perez JE, Klein SC, Prater DM, et al. Automated, on-line quantification of left ventricular dimensions and function by echocardiography with backscatter imaging and lateral gain compensation. Am J Cardiol 1992;70: 1200-5.

28. Perez JE, Waggoner AD, Davila-Roman VG, Cardona H, Miller JG. On-line quantification of ventricular function during dobutamine stress echocardiography. European Heart J 1992;13:1669-76.

29. Madaras EI, Barzilai B, Perez JE, Sobel BE, Miller JG. Changes in myocardial backscatter throughout the cardiac cycle. Ultrasonic Imaging 1983;5:229-39.

30. Collins SM, Skorton DJ, Prasad NV, Olshansky B, Bean JA. Quantitative echocardiographic image texture: normal contraction-related variability. IEEE Trans Med Imag 1985;MI-4:185-92.

31. Fitzgerald PJ, McDaniel MM, Rolett EL, James DH, Strohbehn JW. Two-dimensional ultrasonic variation in myocardium throughout the cardiac cycle. Ultrasonic Imaging 1986;8:241-51.

32. Olshansky B, Collins SM, Skorton DJ, Prasad NV. Variation of left ventricular myocardial gray level on two-dimensional echocardiograms as a result of cardiac contraction. Circ 1984;70:972-7.

33. Barzilai B, Madaras EI, Sobel BE, Miller JG, Perez JE. Effects of myocardial contraction on ultrasonic backscatter before and after ischemia. Am J Physiol 1984; 247(3 Pt 2):H478-H483.

34. Glueck RM, Mottley JG, Miller JG, Sobel BE, Perez JE. Effects of coronary artery occlusion and reperfusion on cardiac cycle-dependent variation of myocardial ultrasonic backscatter. Circ Res 1985;56:683-9.

35. Wickline SA, Thomas LJ III, Miller JG, Sobel BE, Perez JE. The dependence of myocardial ultrasonic integrated backscatter on contractile performance. Circ 1985; 72:183-92.

36. Wickline SA, Thomas LJ III, Miller JG, Sobel BE,

Perez JE. Sensitive detection of the effects of reperfusion on myocardium by ultrasonic tissue characterization with integrated backscatter. Circ 1986;74:389-400.

37. Wear KA, Milunski MR, Wickline SA, Perez JE, Sobel BE, Miller JG. The effect of frequency on the magnitude of cyclic variation of backscatter in dogs and implications for prompt detection of acute myocardial ischemia. IEEE Trans Ultrason Ferroelec Freq Contr 1991; 38:498-502.

38. Fitzgerald PJ, McDaniel MD, Rolett EL, Strohbehn JW, James DH. Two-dimensional ultrasonic tissue characterization: backscatter power, endocardial wall motion, and their phase relationship for normal, ischemic, and infarcted myocardium. Circ 1987;76:850-9.

39. Sagar KB, Rhyne TL, Warltier DC, Pelc L, Wann LS. Intramyocardial variability in integrated backscatter: effects of coronary occlusion and reperfusion. Circ 1987; 75:436-42.

40. Mottley JG, Glueck RM, Perez JE, Sobel BE, Miller JG. Regional differences in the cyclic variation of myocardial backscatter and modification by ischemia. Ultrasonic Imaging (abstr) 1983;5:183.

41. Mottley JG, Glueck RM, Perez JE, Sobel BE, Miller JG. Regional differences in the cyclic variation of myocardial backscatter that parallel regional differences in contractile performance. J Acoust Soc Amer 1984;76: 1617-23.

42. Vered Z, Barzilai B, Mohr GA, et al. Quantitative ultrasonic tissue characterization with real-time integrated backscatter imaging in normal human subjects and in patients with dilated cardiomyopathy. Circ 1987;76:1067-73.

43. Madaras EI, Perez J, Sobel BE, Mottley JG, Miller JG. Anisotropy of the ultrasonic backscatter of myocardial tissue: II. measurements *in vivo*. J Acoust Soc Amer 1988; 83:762-9.

44. Milunski MR, Canter CE, Wickline SA, Sobel BE, Miller JG, Perez JE. Cardiac cycle-dependent variation of integrated backscatter is not distorted by abnormal myocardial wall motion in human subjects with paradoxical septal motion. Ultrasound Med Biol 1989;15:311-8.

45. Milunski MR, Mohr GA, Perez JE, et al. Ultrasonic tissue characterization with integrated backscatter: acute myocardial ischemia, reperfusion, and stunned myocardium in patients. Circ 1989;80:491-503.

46. Milunski MR, Mohr GA, Wear KA, Sobel BE, Miller JG, Wickline SA. Early identification with ultrasonic integrated backscatter of viable but stunned myocardium in dogs. Clin Res 1989;37:280A.

47. Vered Z, Mohr GA, Barzilai B, et al. Ultrasound integrated backscatter tissue characterization of remote myocardial infarction in human subjects. J Am Coll Cardiol 1989;13:84-91.

48. Barzilai B, Vered Z, Mohr GA, et al. Myocardial ultrasonic backscatter for characterization of ischemia and reperfusion: relationship to wall motion. Ultrasound Med Biol 1990;16:391-8.

49. Perez JE, McGill JB, Santiago JV, et al. Abnormal myocardial acoustic properties in diabetic patients and their correlation with the severity of disease. J Am Coll Cardiol 1992;19:1154-6.

50. Hopkins WE, Waggoner AD, Gussak H. Quantitative ultrasonic tissue characterization of myocardium in cyanotic adults with an unrepaired congenital heart defect. Am J Cardiol 1994;74:930-4.

51. Lythall DA, Logan-Sinclair RB, Ilsley CJ, Kushwaha SS, Yacoub MH, Gibson DG. Relation between cyclic variation in echo amplitude and segmental contraction in normal and abnormal hearts. Br Heart J 1991;66: 268-76.

52. Lythall DA, Gibson DG, Kushwaha SS, Norell MS, Mitchell AG, Ilsley CJ. Changes in myocardial echo amplitude during reversible ischaemia in humans. Br Heart J 1992;67:368-76.

53. Masuyama T, St. Goar FG, Tye TL, Oppenheim G, Schnittger I, Popp RL. Ultrasonic tissue characterization of human hypertrophied hearts in vivo with cardiac cycle-dependent variation in integrated backscatter. Circ 1989;80:925-34.

54. Masuyama T, Nellessen U, Schnittger I, Tye TL, Haskell WL, Popp RL. Ultrasonic tissue characterization with a real time integrated backscatter imaging system in normal and aging human hearts. J Am Coll Cardiol 1989; 14:1702-8.

55. Masuyama T, Valantine HA, Gibbons R, Schnittger I, Popp RL. Serial measurement of integrated ultrasonic backscatter in human cardiac allografts for the recognition of acute rejection. Circ 1990;81:829-39.

56. Milunski MR, Mohr GA, Wear KA, Sobel BE, Miller JG, Wickline SA. Early identification with ultrasonic integrated backscatter of viable but stunned myocardium in dogs. J Am Coll Cardiol 1989;14:462-71.

57. Vandenberg BF, Stuhlmuller JE, Rath L, et al. Diagnosis of recent myocardial infarction with quantitative backscatter imaging: preliminary studies. J Am Soc Echo 1991;4:10-8.

58. Loomis JF Jr., Waggoner AD, Schechtman KB,

Miller JG, Sobel BE, Perez JE. Ultrasonic integrated backscatter 2-d imaging: evaluation of M-mode guided acquisition and immediate analysis in 55 consecutive patients. J Am Soc Echo 1990;3:255-65.

59. Eaton MH, Lappas D, Waggoner AD, Perez JE, Miller JG, Barzilai B. Ultrasonic myocardial tissue characterization in the operating room: initial results using transesophageal echocardiography. J Am Soc Echo 1991; 4:541-6.

60. Stuhlmuller JE, Skorton DJ, Burns TL, Melton HEJ, Vandenberg BF. Reproducibility of quantitative backscatter echocardiographic imaging in normal subjects. Am J Cardiol 1992;69:542-6.

61. Brandenburger GH, Klepper JR, Miller JG, Snyder DL. Effects of anisotropy in the ultrasonic attenuation of tissue on computed tomography. Ultrasonic Imaging 1981;3:113-43.

62. Madaras EI, Perez JE, Sobel BE, Miller JG. Anisotropy of ultrasonic backscatter in canine myocardium: results in vivo. Ultrasonic Imaging 1986;8:35-6.

63. Mottley JG, Miller JG. Anisotropy of ultrasonic attenuation in canine heart and liver (abstr). Ultrasonic Imaging 1982;4:180.

64. Mottley JG, Miller JG. Anisotropy of the ultrasonic attenuation in soft tissues: measurements in vitro. J Acoust Soc Amer 1990;88:1203-10.

65. Mottley JG, Miller JG. Anisotropy of ultrasonic backscatter in canine myocardium: theory and results in vitro (abstr). Ultrasonic Imaging 1986;8:34-5.

66. Verdonk ED, Wickline SA, Miller JG. Anisotropy of ultrasonic velocity and elastic properties in normal human myocardium. J Acoust Soc Amer 1992;92:3039-50.

67. Hoffmeister BK, Wong AK, Verdonk ED, Wickline SA, Miller JG. Comparison of the anisotropy of apparent integrated ultrasonic backscatter from fixed human tendon and fixed human myocardium. J Acoust Soc Amer 1995;97:1307-13.

68. Hoffmeister BK, Verdonk ED, Wickline SA, Miller JG. Effect of collagen on the anisotropy of quasi-longitudinal mode ultrasonic velocity in fibrous soft tissues: a comparison of fixed tendon and fixed myocardium. J Acoust Soc Amer 1994;96:1957-64.

69. Vandenberg BF, Rath L, Shoup TA, Kerber RE, Collins SM, Skorton DJ. Cyclic variation of ultrasound backscatter in normal myocardium is view dependent: clinical studies with a real-time backscatter imaging system. J Am Soc Echo 1989;2:308-14.

70. Finch-Johnston AE, Gussak HM, Mobley J, et al. Effect of time delay on the apparent magnitude of cyclic variation of myocardial ultrasonic backscatter in standard echocardiographic views (abstr). Ultrasonic Imaging 1995; 17:77.

71. Ota T, Heinle SK, Evans W, Higgenbotham M, Kisslo J. Echocardiographic cardiac rejection surveillance using acoustic densitometry of two dimensional ultrasound backscatter imaging: multiple views and regions of interest (abstr). J Am Coll Cardiol 1995;25:289A.

72. Wagner RF, Wear KA, Perez JE, McGill JB, Schechtman KB, Miller JG. Quantitative assessment of myocardial ultrasound tissue characterization through receiver operating characteristic analysis of bayesian classifiers. J Am Coll Cardiol 1995;25:1706-11.

73. Mohr GA, Vered Z, Barzilai B, Perez JE, Sobel BE, Miller JG. Automated determination of the magnitude and time delay ("phase") of the cardiac cycle dependent variation of myocardial ultrasonic integrated backscatter. Ultrasonic Imaging 1989;11:245-59.

74. Mobley J, Feinberg MS, Gussak HM, Banta CE, Perez JE, Miller JG. On-line implementation of algorithm for determination of magnitude and time delay of cyclic variation of integrated backscatter in an echocardiographic imager (abstr). Ultrasonic Imaging 1994;16:49.

75. This instability in the magnitude calculation was observed in our lab at Washington University in St. Louis, as well as in the lab of Hans Rijsterborgh and colleagues at Erasmus University, Rotterdam.

76. Thomas LJ III, Wickline SA, Perez JE, Sobel BE, Miller JG. A real-time integrated backscatter measurement system for quantitative cardiac tissue characterization. IEEE Trans Ultrason Ferroelec Freq Contr 1986;UFFC-33:27-32.

77. Thomas LJ III, Barzilai B, Perez JE, Sobel BE, Wickline SA, Miller JG. Quantitative real-time imaging of myocardium based on ultrasonic integrated backscatter. IEEE Trans Ultrason Ferroelec Freq Contr 1989;UFFC-36:466-70.

Video Journal of Echocardiography, Vol. 5, No. 2, pp. 40-48, April 1995

Clinical tissue characterization: online determination of magnitude and time delay of myocardial backscatter

Joel Mobley, MA, Christina E. Banta, MS, Hiie M. Gussak, MD, Julio E. Perez, MD and James G. Miller, PhD

Implementation of an algorithm for the automated determination of the magnitude and time delay of the cardiac cycle-dependent variation of integrated backscatter is reported. This algorithm has been implemented in the experimental firmware of a commercially-available echocardiographic imaging system. Integrated backscatter and the cardiac cycle-dependent variation (cyclic variation) of integrated backscatter are described and their roles in myocardial tissue characterization are discussed. A brief description of the algorithm used for the determination of the magnitude and time delay is given, followed by accounts of the process of collecting cyclic variation data and the algorithm implementation on the cardiac system. This implementation demonstrates how tissue characterization techniques could be used to augment diagnostic ultrasound and may facilitate the further investigation of the diagnostic potential of the cyclic variation of myocardial backscatter.